

OPTIMUM SHAPE CONTROL OF FLEXIBLE BEAMS
BY PIEZO-ELECTRIC ACTUATORS

NAG-520 ----- NAG-749

by

A.Baz and S.Poh
Mechanical Engineering Department
The Catholic University of America
Washington, D.C. 20064

ACKNOWLEDGEMENTS

Special thanks are due to the Space Science and Technology branch at NASA Goddard Space Flight Center for providing the funds necessary to conduct this study under grants number NAG-520 and NAG-749.

Thanks are particularly due to Dr. Joseph Fedor, code 712, for his invaluable engineering inputs which have been crucial to the implementation of this effort.

Special thanks are also due to Mr. Eric Osborne, code 716, for his continuous thought stimulating discussions.

NOMENCLATURE

b	width of beam and piezo-actuator, m
d	electric charge constant of piezo-actuator, m/v
D	distance to neutral axis of composite beam measured from its lower edge, m
$E_{1,2,3}$	Young's modulus of elasticity of piezo-actuator and beam respectively, N/m ²
E_i	Young's modulus of elasticity of element i of the beam, N/m ²
F	vector of external forces and moments, N or Nm
$I_{1,2,3}$	area moment of inertia of actuator, bonding layer and beam about the neutral axis of the composite beam respectively, m ⁴
I_i	area moment of inertia of the element i , m ⁴
K_i	stiffness matrix of the element i
K	overall stiffness matrix of beam-actuator system
l_i	length of element i , m
M_{ei}	external moment acting on i^{th} node of beam, Nm
M_f	piezo-electric moment generated by piezo-film, Nm
N	number of elements of the beam
$t_{1,2,3}$	thickness of piezo-actuator, bonding layer and beam respectively, m
U	deflection criterion
v	voltage applied across the piezo-electric film, volts
V_i	external force acting on the i^{th} element of the beam, N
Y_i	the linear translation of node i , m

Greek Letters

δ_i	deflection of node i, m or rad.
δ	deflection vector of all nodes of the beam, m or rad.
ϵ_f	piezo-electric strain in piezo-actuator, m/m
$\sigma_{1,2,3}$	bending stresses in piezo-actuator, bonding layer and beam respectively, N/m ²
σ_f	piezo-electric stress in actuator, N/m ²

ABSTRACT

This study deals with the utilization of piezo-electric actuators in controlling the static deformation and shape of flexible beams.

An optimum design procedure is presented to enable the selection of the optimal location, thickness and excitation voltage of the piezo-electric actuators in a way that would minimize the deflection of the beam to which these actuators are bonded.

Numerical examples are presented to illustrate the application of the developed optimization procedure in minimizing structural deformation of beams using ceramic and polymeric piezo-electric actuators bonded to the beams with a typical bonding agent.

The obtained results emphasize the importance of the devised rational produce in designing beam-actuator systems with minimal elastic distortions.

INTRODUCTION

The construction and operation of large structures which are extremely flexible have posed new and challenging problems particularly because these structures are intended to provide stable bases for observations and communications such as in space structures. With strict constraints imposed on the structural deformations, it became essential to suppress such deformations to minimum through the use of active control systems of one form or another.

Distinct among the presently available active control systems are those that rely in their operation on piezo-electric actuators. Such systems have proven to be experimentally effective in controlling the vibrations of simple structural elements such as rectangular beams [1-2] and hollow cylindrical masts [3]. The effectiveness of these systems is coupled also with the light weight, high force and low power consumption capabilities of the piezo-electric actuators [4-8]. These features rendered this class of actuators to be an attractive candidate for controlling structural deformation.

The present state-of-the-art of this type of actuators has been limited to the analysis and testing of their characteristics [9-11] as influenced by their geometrical or operational conditions. But, no attempt has been made towards selecting their optimal geometrical parameters or location which are suited for a

particular structure subjected to known loading conditions. Such a synthesis procedure is essential to the successful integration of the actuators into the structure in order to minimize the structural deformation.

It is, therefore, the purpose of this study to devise such an optimal design procedure that would enable the selection, on rational basis, of the optimum design parameters and location of piezo-electric actuators to satisfy certain structural deformation requirements. The procedure will take into account the effect that the actuators have on changing the elastic and inertial properties of the structure to which they are bonded to. Furthermore, it considers the effect of physical and geometrical properties of the bonding layer on the static characteristic of the beam-actuator system.

THE PIEZO-ELECTRIC ACTUATOR-BEAM SYSTEM

A. General Layout

Figure (1) shows a general layout of a flexible beam (A) whose deflection is to be controlled by piezo-electric actuator (B) bonded to the beam by bonding layer (C). The beam, under consideration, can generally be made of several steps which are not necessarily of the same thickness or the same material. The interfacial nodes between the different steps can be subjected to

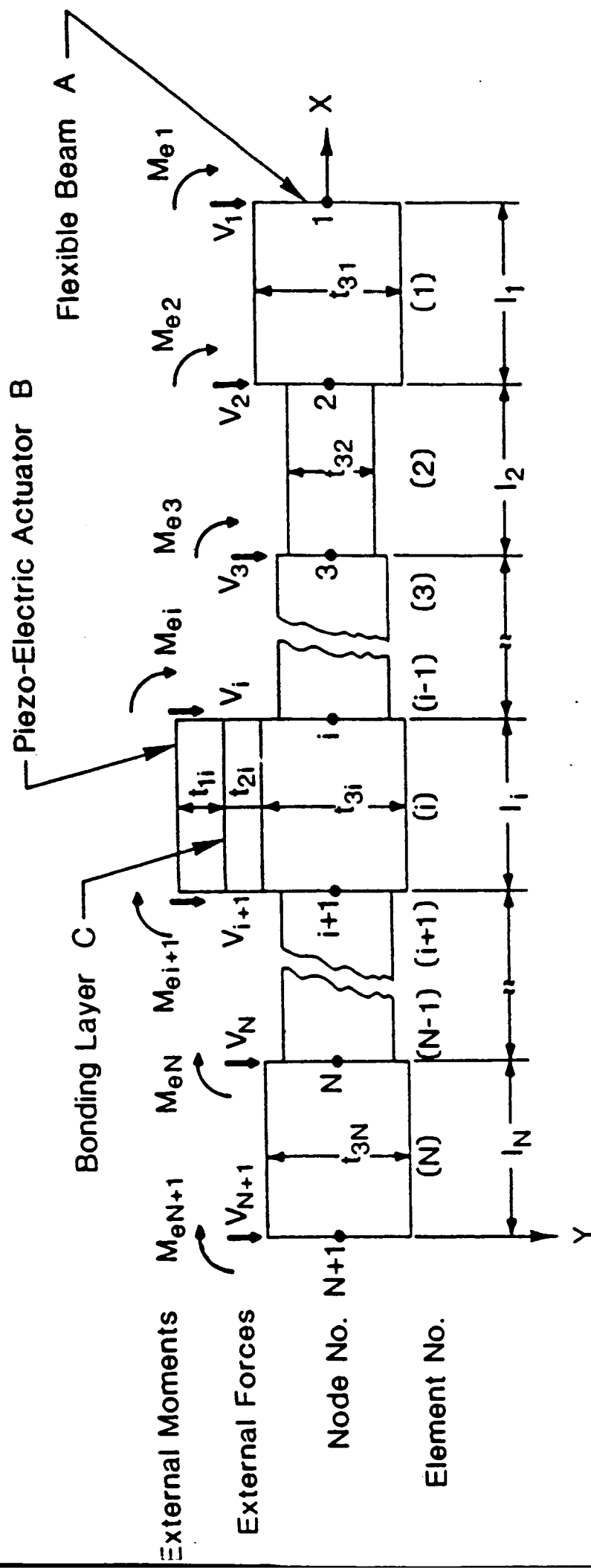


Figure (1) - General layout of the piezo-electric actuator-beam system.

external forces, moments or both. Further, the degrees of freedom of any node can be limited to linear translations, angular rotations or restrained completely depending on the nature of support at the node under consideration.

In this study, the beam is assumed to have rectangular cross section of constant width b and that its transverse deflection is due to the flexural action of the external forces and moments.

In Figure (1), the piezo-electric actuator B is shown bonded to the element i of the flexible beam to form a composite beam. When an electric field is applied across the film, then it will expand if the field is, for example, along the polarization axis of the film and will contract if the two were out of phase. The expansion or contraction of the film relative to the beam, by virtue of the piezo-electric effect, creates longitudinal bending stresses in the composite beam which tend to bend the beam in a manner very similar to a bimetallic thermostat.

With proper selection, placement and control of the actuator, it would be possible to generate enough piezo-electric bending stresses to counter balance the effect of the exciting forces and moments acting on the beam in a way that minimizes its structural vibrations.

B. Model Of An Actuator-Beam Element

Figure (2) shows a schematic drawing of a piezo-film A bonded to an element B of the flexible beam.

If a voltage v is applied across the film, a piezo-electric strain ϵ_f is introduced in the film and can be computed from :

$$\epsilon_f = (d/t_1)*v \quad (1)$$

where d is the electric charge constant of the film, m/v
 t_1 is the thickness of the piezo-electric actuator, m

This strain results in a longitudinal stress σ_f given by :

$$\sigma_f = E_1(d/t_1)*v \quad (2)$$

where E_1 is the Young's modulus of elasticity of the film, N/m^2
 This, in turn generates a bending moment M_f , around the neutral axis of the composite beam, given by :

$$M_f = \frac{-(t_1+t_2+t_3-D)}{-(t_2+t_3-D)} \int \sigma_f(b*y)dy \quad (3)$$

where t_2 is the thickness of the bonding layer, m
 t_3 is the thickness of the beam, m
 b is the width of the beam, the bonding layer and the piezo-film, m

In equation (3), D is the distance of the neutral axis from the lower edge of the beam which can be determined by considering the force balance in the longitudinal direction X of the beam, or :

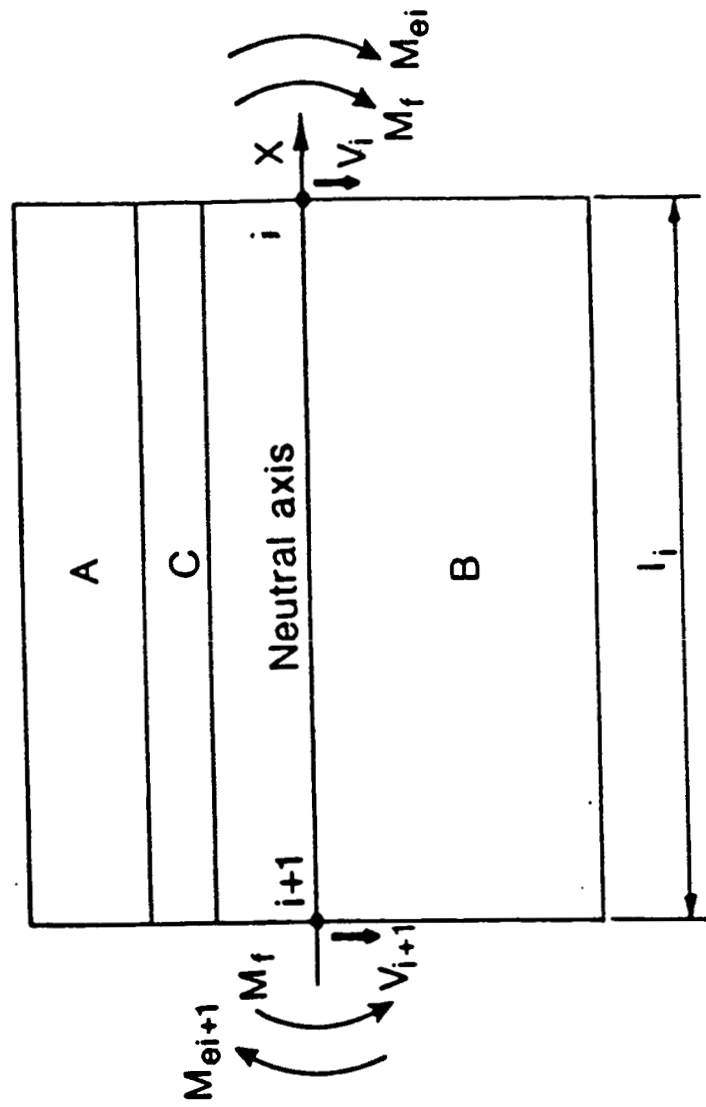
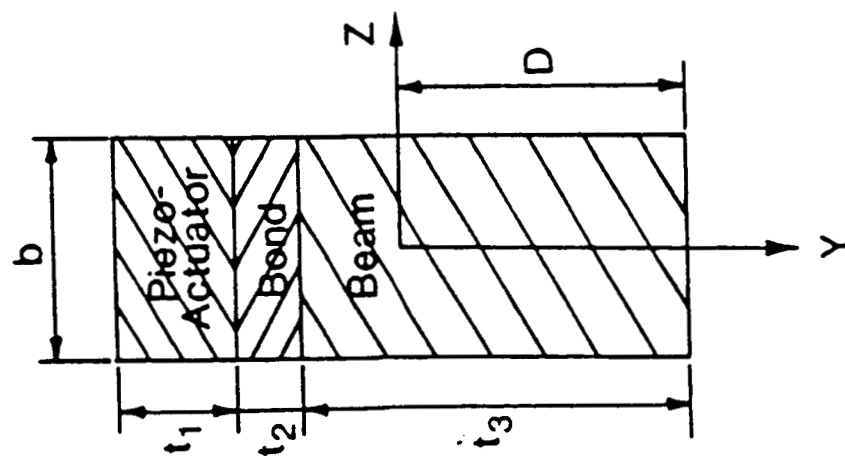


Figure (2) - Schematic drawing of an actuator bonded to a flexible beam element.

$$\int_{\text{film}} \sigma_1 dA + \int_{\text{bond}} \sigma_2 dA + \int_{\text{beam}} \sigma_3 dA = 0 \quad (4)$$

or

$$E_1 b \int_{-(t_1+t_2+t_3-D)}^{-(t_2+t_3-D)} y dy + E_2 b \int_{-(t_2+t_3-D)}^{-(t_3-D)} y dy + E_3 b \int_{-(t_3-D)}^D y dy = 0 \quad (5)$$

where E_2 is Young's modulus of elasticity of the bonding layer

E_3 is Young's modulus of elasticity of the beam

Equation (5) yields the following expression for D :

$$D = \frac{E_1 t_1^2 + E_2 t_2^2 + E_3 t_3^2 + 2E_1 t_1(t_2 + t_3) + 2E_2 t_2 t_3}{2(E_1 t_1 + E_2 t_2 + E_3 t_3)} \quad (6)$$

Equation (2), (3) and (6) can be combined to determine the bending moment M_f generated by the piezo-film on the composite beam as follows :

$$M_f = \frac{d \cdot b \cdot E_1 \cdot v \cdot (E_2 t_1 t_2 + E_3 t_1 t_3 + E_2 t_2^2 + 2E_3 t_2 t_3 + E_3 t_3^2)}{2 \cdot (E_1 t_1 + E_2 t_2 + E_3 t_3)} \quad (7)$$

For this composite beam, it can be easily shown [12] that it has a flexural rigidity ($E_1 I_1$) given by :

$$E_1 I_1 = E_1 I_1 + E_2 I_2 + E_3 I_3 \quad (8)$$

where I_1 , I_2 and I_3 are the area moments of inertia of the film, the bonding layer and the beam about the neutral axis respectively.

Let us now assume that the composite beam, shown in Figure

(2), extends a length l_i between two nodes (i) and (i+1). Further, it is assumed that the external forces V_i and V_{i+1} as well as the external moments M_{ei} and M_{ei+1} are acting on the beam at nodes i and i+1 respectively. Then, the resulting linear and angular deformations of the beam y_i and θ_i as well as y_{i+1} and θ_{i+1} at the nodes i and i+1, respectively, can be related to the loads acting on the element as follows [13] :

$$\begin{bmatrix} V_i \\ M_{ei}+M_f \\ V_{i+1} \\ M_{ei+1}-M_f \end{bmatrix} = \frac{E_i I_i}{L_i^3} \begin{bmatrix} 12 & 6L_i & -12 & 6L_i \\ 6L_i & 4L_i^2 & -6L_i & 2L_i^2 \\ -12 & -6L_i & 12 & -6L_i \\ 6L_i & 2L_i^2 & -6L_i & 4L_i^2 \end{bmatrix} \begin{bmatrix} y_i \\ \theta_i \\ y_{i+1} \\ \theta_{i+1} \end{bmatrix} \quad (9)$$

Equation (9) can be rewritten as :

$$F_i = K_i \delta_i \quad (10)$$

where F_i is the resultant forces and moments vector acting on the beam element i, N

K_i is the stiffness matrix of the composite beam element i, N/m

δ_i is the deflection vector of the nodes bounding the beam element, m

Equation (9) constitutes the basic finite element model that relates the external loads (V and M_e) and piezo-electric moments (M_f) to the deflections (y and θ) of the element as a function of its elastic and inertial parameters.

The equation can be equally used for any element of the beam whether it has a piezo-film bonded to it or not. In the latter case, M_f is set to zero and flextural rigidity $E_i I_i$ is set equal to that of the flexible beam element under consideration.

C. Model Of The Overall Actuator-Beam System

The force-displacement characteristics of the individual elements of the beam-actuator system, as given for element i by equation (9), are combined to determine the behavior of the overall structure.

The equilibrium conditions of the overall structure will be expressed as :

$$\begin{array}{l} \text{External forces and moment} \\ \text{acting on the nodes} \\ \text{of the overall system} \end{array} = \sum \begin{array}{l} \text{forces and moments} \\ \text{acting on the elements} \\ \text{at these nodes} \end{array}$$

or

$$F = \sum_{i=1}^{N+1} F_i = \sum_{i=1}^{N+1} K_i \delta_i = K \delta \quad (11)$$

where K is the overall stiffness matrix of the system ($2n \times 2n$)

Bathe and Wilson [14], Yang [15] and Fenner [16], for example, show how to generate the overall matrix K from the stiffness matrices K_i of the individual elements.

In equation (11), the external force vector F and the

displacement vector δ are given by:

$$F^T = [V_1 \ M_1 \ V_2 \ M_2 \ \dots \ V_{N+1} \ M_{N+1}] \quad (12)$$

and

$$\delta^T = [Y_1 \ \theta_1 \ Y_2 \ \theta_2 \ \dots \ Y_{N+1} \ \theta_{N+1}] \quad (13)$$

where superscript T denotes the transpose of the vector

D. Solution Algorithm

For a particular flexible beam configuration, external loading conditions and end conditions, the effect of applying certain voltage v on a piezo-electric actuator of a specific thickness t_1 placed at a particular location i on modifying the elastic deflection δ of the beam can be determined by solving equation (11).

In equation (11), the overall stiffness matrix K is modified to account for the end conditions and type of restraints imposed on the different nodes. If, for example, a node (j) is simply-supported and is therefore restrained in the Y direction, i.e. $y_j=0$, then the off diagonal elements of $2*j$ row of the overall stiffness matrix K are set equal to zero together with the corresponding externally applied force. If the j^{th} node is also restrained in its angular motion then $\theta_j=0$ and the off diagonal elements of the $(2*j+1)$ row of the K matrix are eliminated along with the corresponding externally applied moment.

After such a modification process, the elastic deflection of the beam can be computed from :

$$\delta = K^{-1} * F \quad (14)$$

where K^{-1} is the inverse of the overall stiffness matrix

Figure (3) shows a flowchart of the solution algorithm.

OPTIMIZATION OF THE ACTUATOR-BEAM SYSTEM

The presented analysis algorithm of the actuator-beam system is utilized as a basic for the development of the optimization procedure for selecting the thickness t_1 , excitation voltage v and location i of the actuator in order to minimize the deflection of the beam.

The optimum design problem is formulated as follows :

Find thickness t_1 , voltage v and location i

to Minimize $U = \left(\sum_{i=1}^{N+1} (Y_i^2 + \theta_i^2) \right) * b t_1$

Such that

$$V_i = V_i^*$$

$$M_{ei} = M_{ei}^*, \quad i=1, 2, \dots, N+1$$

$$v/t_1 < v^*,$$

$$E_1 dv/t_1 < \sigma^*,$$

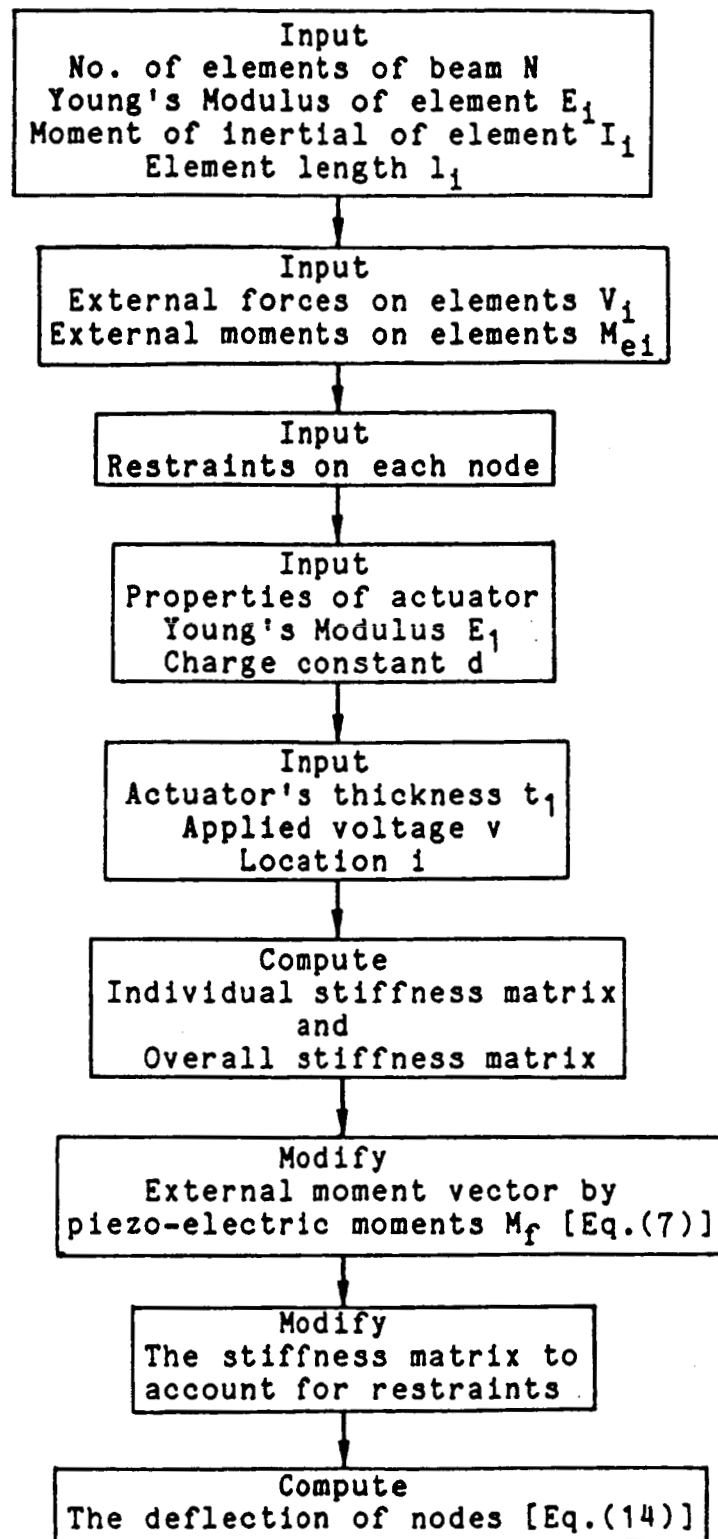


Figure (3) - Flowchart of the solution algorithm

$$\begin{aligned}
t_1 &< t_1^*, \\
v_{\min} &< v < v_{\max}, \\
Y_i &< Y_{\max}, \\
\text{and } \theta_i &< \theta_{\max}
\end{aligned}$$

The considered objective function aims at minimizing the linear and angular deflections of the beam as well as the weight of the piezo-actuator.

Such a formulation results in a nonlinear optimization problem in 3 design variables t_1 , v and i which is subjected to seven inequality constraints. The first inequality constraint guards against the application of a high voltage across the actuator that may result in its depolarization. The second inequality constraint limits the stresses in the piezo-film within the acceptable safe limits defined by the allowable stress σ^* . The last two inequalities limit the linear and angular static distortions to set permissible operational limits.

A penalty function algorithm is used to transform the constrained minimization problem into an unconstrained optimization which is solved using a Powell's Conjugate Direction method [17].

Figure (4) shows a block diagram of the optimization algorithm.

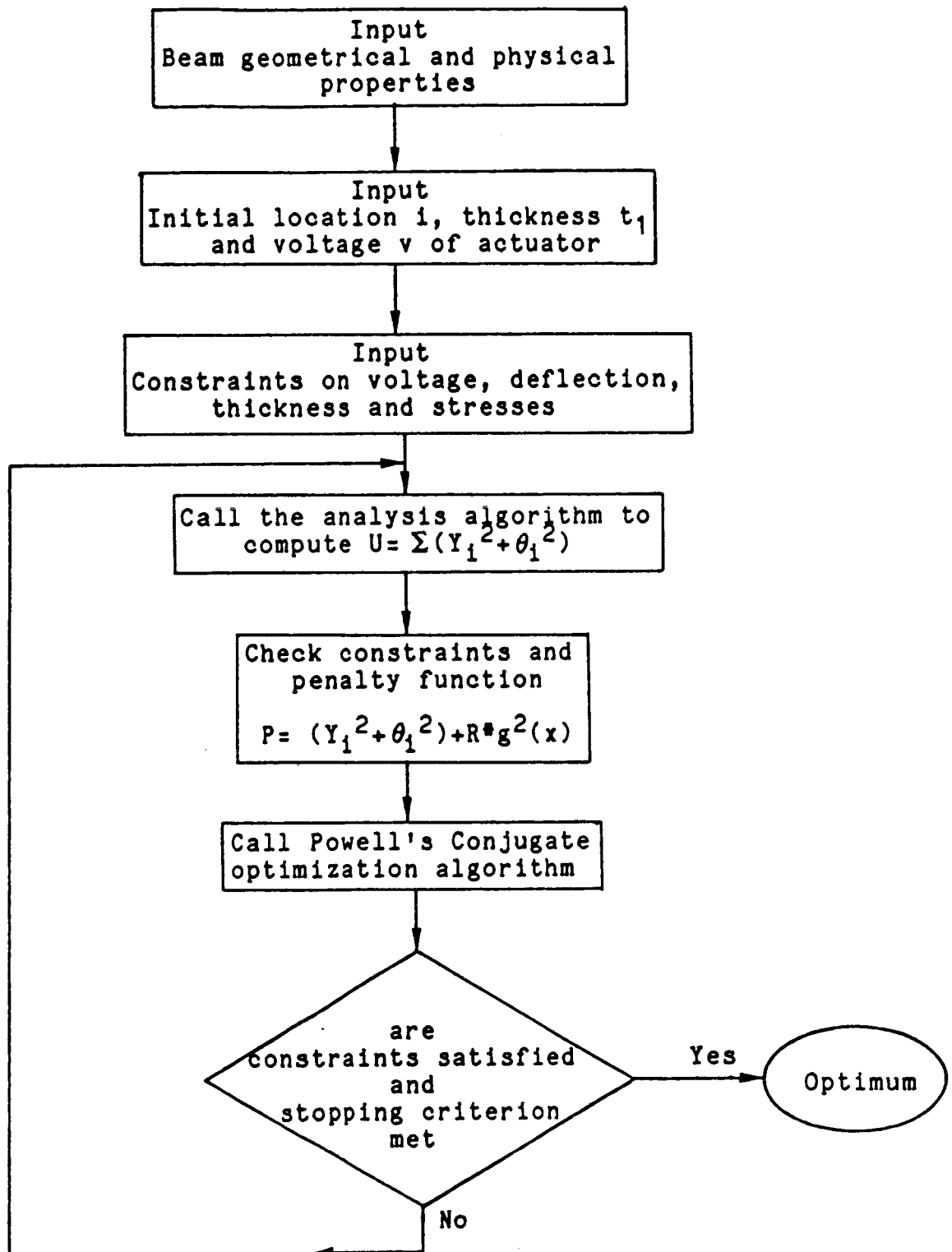


Figure (4) - Flowchart of the optimization algorithm

NUMERICAL EXAMPLES

The developed optimization procedure is used to optimally select, place and control the action of a single piezo-electric actuator bonded to a three-element straight steel cantilever beam, shown in Figure (5), that is 0.0125m wide, 0.0021m thick and 0.15m long. The effect of physical properties of the piezo-actuator and the bonding layer on the optimal configuration of the system is presented.

The physical properties of the considered piezo-actuators and a typical bonding material are given in Tables (1) and (2) respectively.

A. Performance With PZT Actuator

(i) neglecting the effect of bonding layer

Figure (6) displays a 2-D plot of the design space in the t_1 - v plane of the 3-D problem when one PZT piezo-actuator is placed at element 3 near the fixed end of the beam. This plot will give an understanding of the interaction between the constraints and the design objective. Plotted on this plane are the objective function contours and the constraints along with a search path to the optimum from a selected starting point. For such a case, the objective function assumes a minimum of

Table (1) - Properties of piezo-electric actuators

Actuator type	Ceramic [Ref.8]	Polymeric [Ref.18]
Material	PZT	Kynar (PVF2)
Charge coefficient d 10^{-12} (m/v)	123	23
Young's modulus (G N/m ²)	139	2
Max. voltage v* (Mv/m)	1	30
Max. tensile strength * (M N/m ²)	45	33-55
Density (kg/m ³)	7500	1780

Table (2) - Properties of a typical bonding layer [Ref.10]

Bonding Layer	Density (Kg/m ³)	Young's Modulus (MN/m ²)
Eastman 910 ¹	1050	1780.0

1 Cyanoacrylate adhesive made by eastman Kodak Co., Rochester, NY

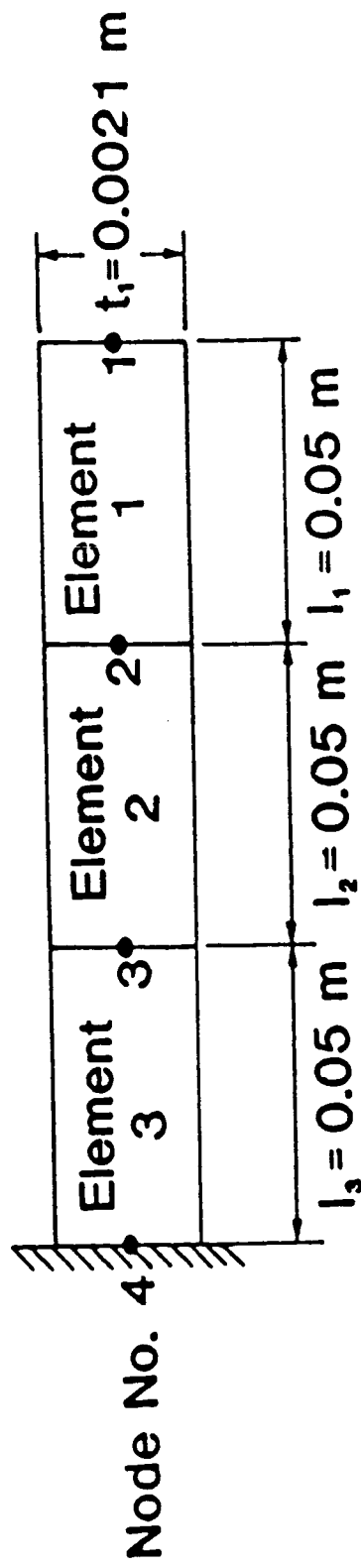


Figure (5) - Schematic drawing of a three-element cantilever beam

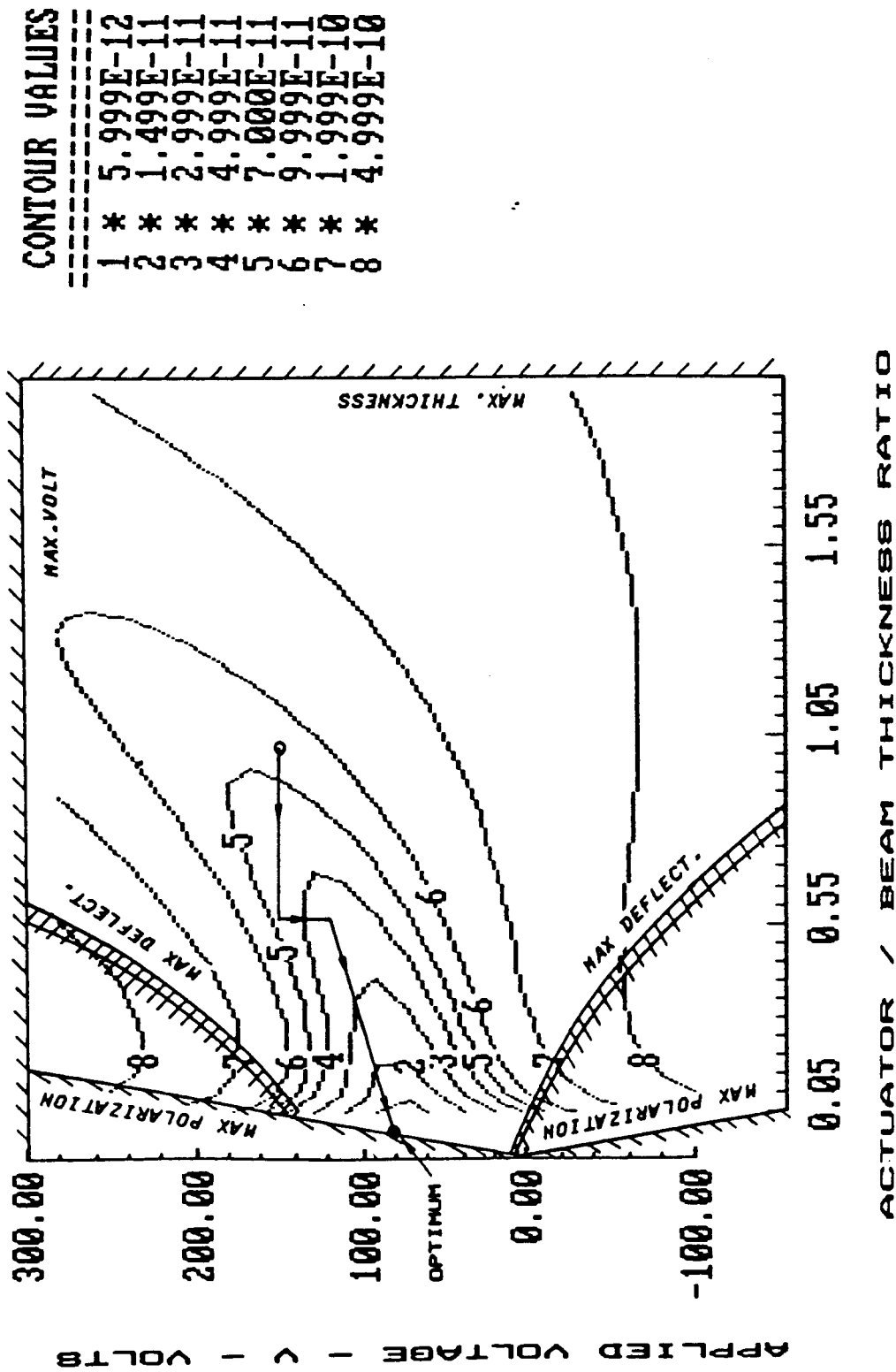


Figure (6) - Iso-objective function contours with one PZT actuator placed at element 3 neglecting effect of bond ($V^* = 10^6 \text{ V/m}$, $\sigma^* = 45 \text{ MN/m}^2$, $t_1^* = 0.0084 \text{ m}$, $V_{\text{max}} = 300 \text{ V}$, $Y_{\text{max}} = 0.00005 \text{ m}$ and $\theta_{\text{max}} = 0.0005 \text{ rad}$.)

2.74×10^{-12} when a 0.08mm thick PZT actuator is placed at element 3 and is energized by 80.00 volts. It can be seen that the optimum point lies, for the considered case and constraints, on the polarization constraint.

Now to gain an insight into the effect that third dimension, i.e. the actuator location, has on the deflection characteristics of the beam let us consider the profiles of the different elastic lines obtained by varying the location of the actuator. The linear and angular elastic deformation are shown in Figures (7-a) and (7-b) respectively for both the uncontrolled and controlled beams. It is evident from the figures that placing an actuator at element 1 produced the least compensation for the external loads and its effects are limited to the first element only. However, placing the actuator at the third element, near the fixed end, results in considerable improvement that is not confined to element 3 is manifested clearly all over the three elements.

(ii) Considering the effect of bonding layer

When the elastic and inertial properties of the bonding layer are accounted for, then the optimum values of the voltage, thickness of PZT actuator and the objective function are as shown in Figure (8) as function of the thickness of the bonding layer. The displayed results are obtained with Eastman 910 as the bonding layer. The figure indicates that increasing the thickness of the bonding layer results in reducing the optimum values of

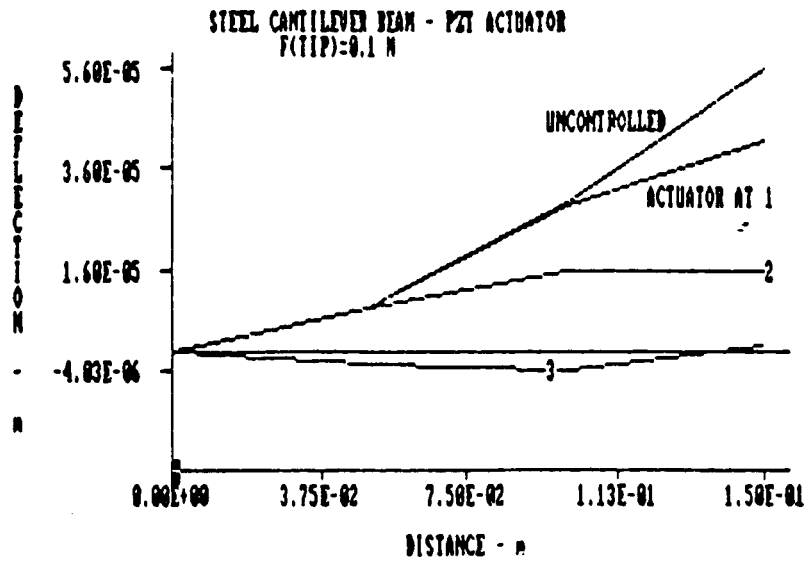


Figure (7-a) - Effect of placement strategy of a PZT actuator on the linear deflection of the beam

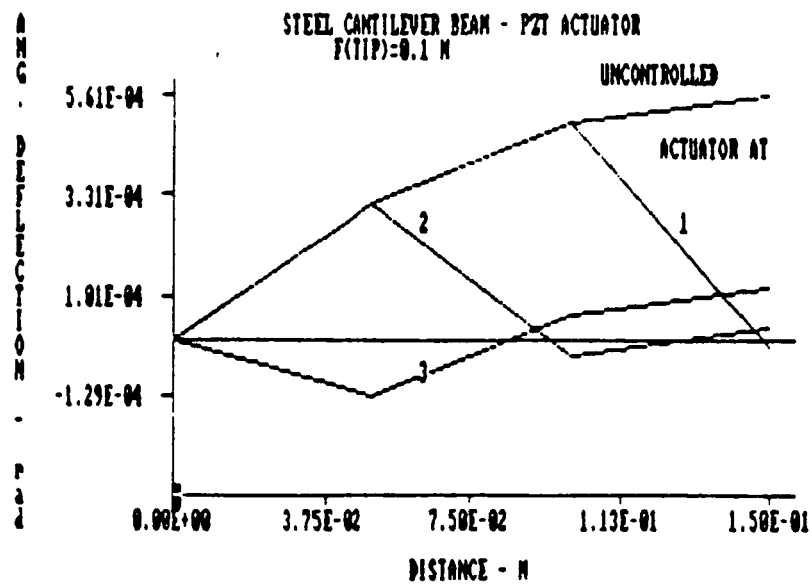


Figure (7-b) - Effect of placement strategy of a PZT actuator on the angular deflection of the beam

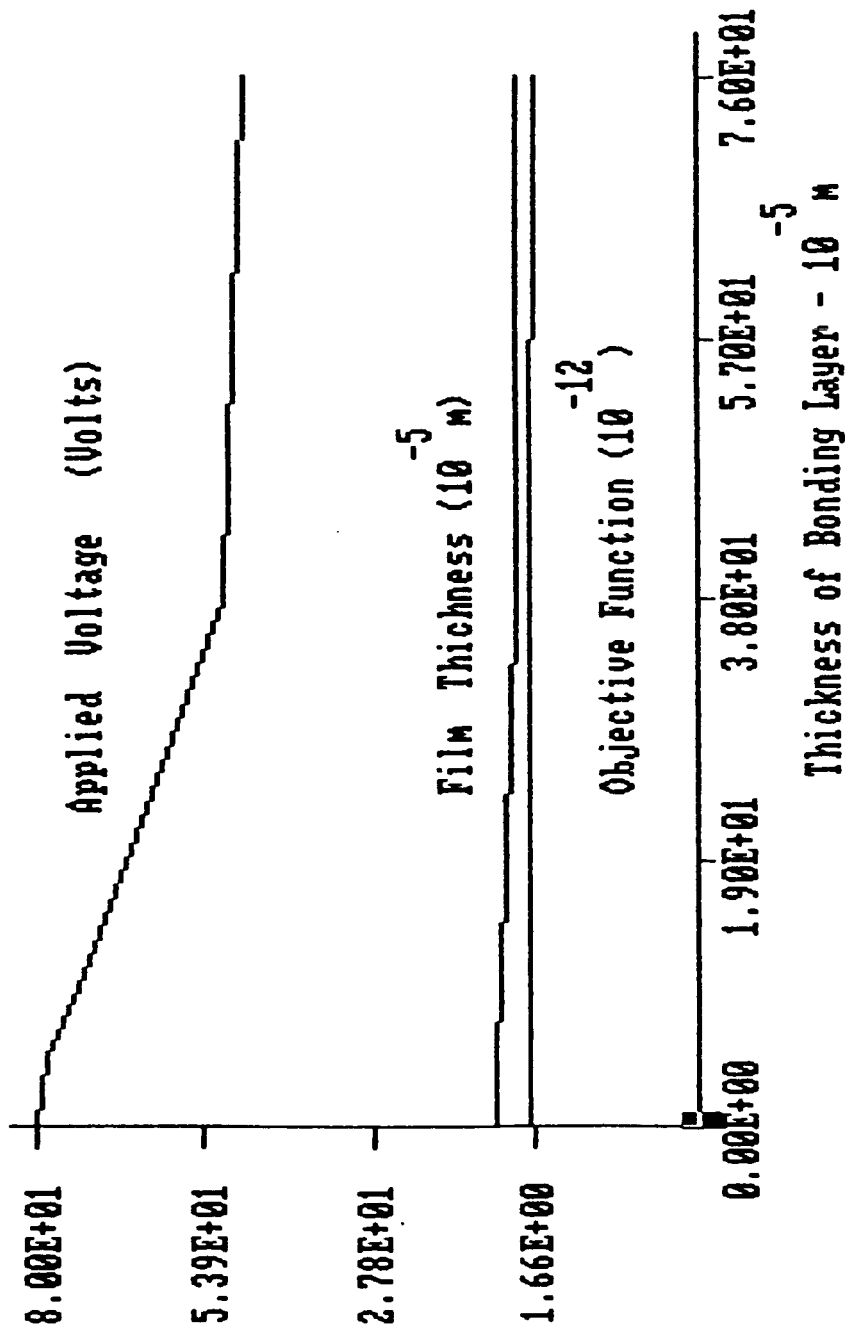


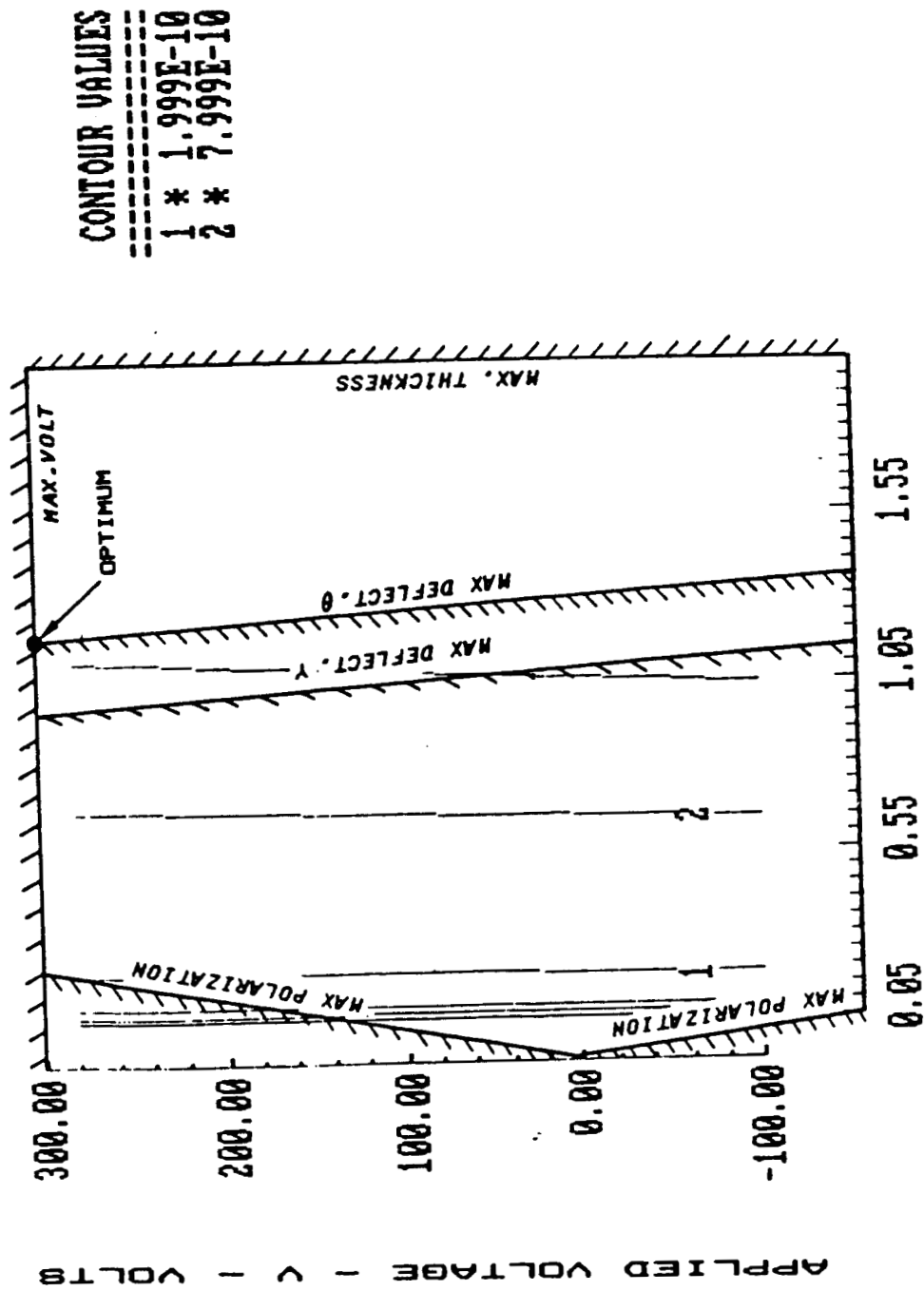
Figure (8) - Effect of thickness of bonding layer on the optimum values of the applied voltage, actuator thickness and objective function when using one PZT actuator ($V^* = 10^6 \text{ V/m}$, $\sigma^* = 45 \text{ MN/m}^2$, $t_1^* = 0.0084 \text{ m}$, $v_{\max} = 300 \text{ v}$, $Y_{\max} = 0.00005 \text{ m}$ and $\theta_{\max} = 0.0005 \text{ rad}$.)

both the applied voltage (v) and the actuator thickness (t_1) in a monotonic fashion. This can be attributed to the stiffening effect produced by the addition of bonding layer to the actuator-beam system as measured by the augmented flexible rigidity, computed from equation (8), and the element stiffness matrix given by equation (9). Such an effect results in reducing the deflections of the uncontrolled system. Accordingly, smaller voltages and actuator thickness would be needed to compensate for these reduced deflections. The figure indicates, however, that the effect of bonding layer on the optimal parameters v and t_1 starts to level off beyond certain bonding layer thickness t_2 of 0.00038m. This is due to the fact that the increased flexural rigidity of the composite is accompanied by a corresponding increase in the piezo-electric moment M_f as given by equation (7). Therefore, these two factors balance each other to obtain a minimum objective function.

B. Performance With Kynar Actuator

Figure (9) shows a projection of the feasible design space in the v - t_1 plane when one Kynar piezo-actuator is placed on element 3 without bond.

The figure indicates that the objective function assumes a minimum of 1.24×10^{-9} when a 0.00244mm thick Kynar actuator is bonded to element 3 and is powered by 300 volts.



ACTUATOR / BEAM THICKNESS RATIO

Figure (9) - Iso-objective function contours with one Kynar actuator placed at element 3 neglecting effect of bond ($V^* = 10^6 \text{ v/m}$, $\sigma^* = 45 \text{ MN/m}^2$, $t_1^* = 0.0084 \text{ m}$, $v_{\text{max}} = 300 \text{ v}$, $\gamma_{\text{max}} = 0.00005 \text{ m}$ and $\theta_{\text{max}} = 0.0005 \text{ rad.}$)

Therefore, under the same conditions and constraint limit, it is seen that the use of kynar actuator results in pushing the optimum towards the maximum voltage constraint instead of the polarization constraint as obtained with PZT actuators. More importantly, the optimum design with the Kynar actuator requires a piezo film which is about 3 times thicker than the optimal PZT film. Furthermore, in spite of the higher voltage and thicker actuator, the attained design objective is almost three orders of magnitudes higher than that obtained with the PZT actuator.

Accordingly, from the v , t_1 and U points of view, the use of the PZT actuator is favored over the Kynar actuator.

Similar trends, to the PZT case, are also observed when the effect of the elastic and inertial properties of the bonding layer are considered as shown in Figure (10).

CONCLUSIONS

This paper has presented an optimum design procedure for controlling the shape of flexible beams using piezo-electric actuators. The procedure is based on accounting for the effect of the physical parameters of the actuator and its bonding layer on the elastic and inertial characteristics of the flexible beam. The presented procedure is utilized to select the voltage, thickness and location of piezo-actuators to minimize the

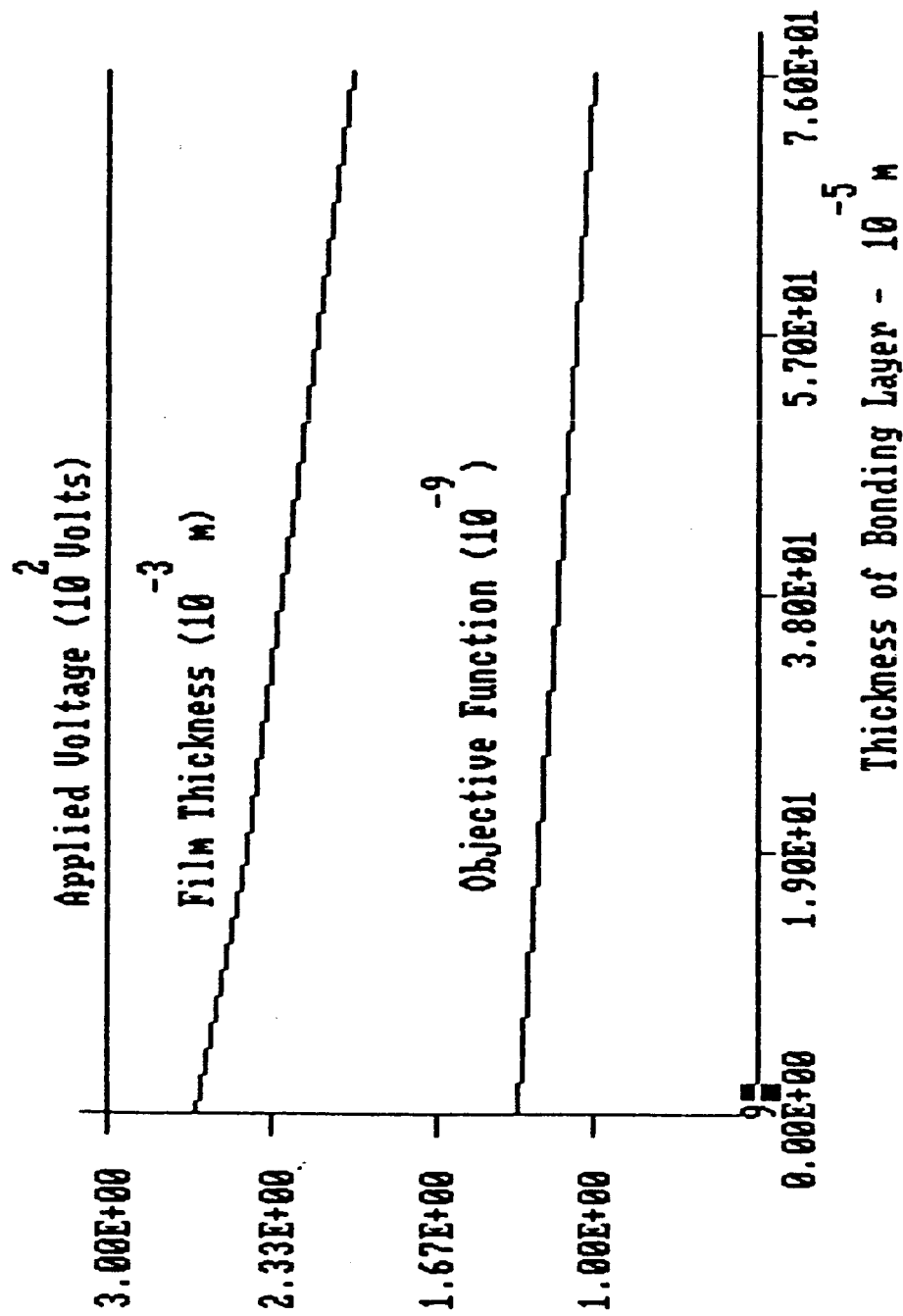


Figure (10) - Effect of thickness of bonding layer on the optimum values of the applied voltage, actuator thickness and objective function when using one Kynar actuator ($V^* = 10^6$ v/m, $\sigma^* = 45$ MN/m², $t_1^* = 0.0084$ m, $v_{\max} = 300$ v, $Y_{\max} = 0.00005$ m and $\theta_{\max} = 0.0005$ rad.)

structural distortion of flexible beams.

The obtained results indicate that ceramic actuators are more effective than polymeric actuators in controlling the shape of a beam with lower voltage and thinner piezo films. Also, it is found that the addition of a bonding layer between the actuator and the beam results in stiffening the actuator-beam system and accordingly reduces the required applied voltage as well as actuator thickness.

REFERENCES

1. Crawley, E.F., and J.de Luis, "Use of piezo-Ceramics as distributed actuators in Large Space Structures", Proc. of the 26th structures, Structure Dynamics and Materials conference, Part 2, AIAA-ASME-ASCE, Orlando-Florida, pp.126-133, April 1985.
2. Bailey, T. and James E.Hubbard Jr., "Distributed Piezo-electric Polymer Active Vibration Control of a Cantilever Beam", J. of Guidance and Control, Vol. 8, No.5, pp. 605-611, Sept.-Oct. 1985.
3. Forward, R.L., "Electronic Damping of Orthogonal Bending Modes in a Cylindrical Mast-Experiment", J. Spacecraft, Vol. 18, No. 1, pp. 11-17, Jan.-Feb. 1981.
4. Lockheed Missiles and Space Company, Inc., "Vibration Control of Space Structures, VCOSS A: High and Low-Authority Hardware Implementations", Report #AFWAL-TR-83-3074, July 1983.
5. Aronson, R.B., (ed.), "Rediscovering Piezoelectrics", Machine Design, Vol. 56, No. 14, pp.73-77, 1984.
6. Toda, M., S. Osaka and E. Johnson, "A new Electromotional Device", RCA Engineer, Vol. 25, No. 1, pp. 24-27, 1979.
7. Toda, M., S. Osaka and S. Tosima, "Large Area Display Element Using PVF2 Bimorph With Double-Support Structure", Ferroelectronics, Vol. 23, pp. 115-120, 1980.
8. Piezo-Electric Products, Inc., "Piezoceramic Design Notes", Sensors, Mar. 1984.
9. Toda, M., "Electromotional Device Using PVF2 Multilayer

Bimorph", Trans. of the IECE of Japan, vol. E61, No. 7, pp. 507-512, July 1978.

10. Kelly Lee, J. and M. Marcus, "The Deflection-Bandwidth Product of PVF Benders and Related Structures", Ferroelectonics, Vol. 32, pp. 93-101, 1981.
11. Toda, M., "Elastic Properties of Piezo-Electric PVF₂", J. Appl. Phys., Vol. 51, No. 9, pp. 4673-4677, Sept. 1980.
12. Gere, J.M and S.P. Timoshenko, "Mechanics of Materials", 2nd Edition, Brooks/Cole Engineering Division, Monterey CA, 1984.
13. Paz, M., "Structural Dynamics : Theory and Computation", 2nd Edition, Van Nostrand Reinhold Co, New York, 1985.
14. Bathe, K.J. and E.L. Wilson, "Numerical Methods in Finite Element Analysis", Prentice-Hall Inc., Englewood Cliffs, NJ, 1976.
15. Yang, T. Y., "Finite Element Structural Analysis", Prentice-Hall Inc., Englewood Cliffs, NJ, 1986.
16. Fenner, R.T., "Finite Element Methods for Engineers", McMillan Press Ltd, London, 1975.
17. Reklaitis, G.V., A. Ravindran and K.M. Ragsdell, "Engineering Optimization : Methods and Applications", J. Wiley and Sons, NY, 1983.
18. Pennwalt Corp., "Kynar Piezo-film", King of Prussia, PA, 19406-0018.